Optimized Switching Between Sensing and Communication for mmWave MU-MISO Systems

Jeongwan Kang[1], Henk Wymeersch[2], Carlo Fischione[3], Gonzalo Seco-Granados[4] and Sunwoo Kim[1]
[1]Department of Electronic Engineering, Hanyang University, Seoul, South Korea
[2]Department of Electrical Engineering, Chalmers University of Technology, Gutenberg, Sweden
[3]Division of Network and Systems Engineering, KTH Royal Institute of Technology, Stockholm, Sweden
[4]Department of Telecommunications and Systems Engineering, Universitat Autonoma de Barcelona, Barcelona, Spain
Email: {rkdwjddhks77,remero}@hanyang.ac.kr, henkw@chalmers.se, carlofi@kth.se, gonzalo.seco@uab.cat

2022 IEEE International Conference on Communications Workshops (ICC Workshops) | 978-1-6654-2671-8/22/$31.00 ©2022 IEEE | DOI: 10.1109/ICCWORKSHOPS53468.2022.9814527

***Abstract*—In this paper, we propose a scheme optimizing the per-user channel sensing duration in millimeter-wave (mmWave) multi-user multiple-input single-output (MU-MISO) systems. For each user, the BS predicts the effective rate to be achieved after pilot transmission. Then, the channel sensing duration of each user is optimized by ending the pilot transmission when the predicted rate is lower than the current rate. The robust regularized zero-forcing (RRZF) precoder and equal power allocation (EPA) are adopted to transmit sensing pilots and data. Numerical results show that the more severe the interference among users, the longer channel sensing duration is required. Moreover, the proposed scheme results in a higher sum rate compared to benchmark schemes.**

***Index Terms*—channel sensing duration, rate prediction, Cramer Rao bound (CRB), integrated sensing and communications (ISAC), mmWave**

I. Introduction

Millimeter-wave (mmWave) communication is one of the key techniques of 5G new radio (NR) and Beyond 5G (B5G) systems to improve the data rates and enable a variety of sensing services [1]. The integrated of sensing and communication (ISAC), comes in different forms, including joint data transmission and mono-static sensing, and pilot transmission for bi-static sensing [2]. In particular, channel estimation can be interpreted as a fundamental integration of bi-static sensing and communication, as knowledge of the channel is prerequisite for beamforming and high-rate directional transmission. However, a large number of pilot transmissions are required for channel estimation [3] and leads to a trade-off between the data rate and channel estimation overhead [4]. Therefore, reducing or optimizing bi-static sensing/channel estimation overhead is a critical challenge to improve the data rate in mmWave communication.

An adaptive scheme optimizing the channel sensing duration has been introduced for the single-user multiple-input multiple-output (SU-MIMO) systems [5]. Before each pilot transmission, the BS predicts the downlink effective rate achieved after the possible pilot transmission, and optimizes the channel sensing duration by comparing the predicted rate with the current rate. However, the base station (BS) communicates with multiple users (UEs) interfering with each other, and precoding and power allocation should be additionally considered. In multi-user multiple-input-single-output (MU-MISO) systems, a few works reducing or optimizing channel sensing duration have been proposed in [6]–[10]. The authors in [6], [7] present a scheme for reducing channel estimation overhead by exploiting the structure of spatial channel correlation or using minimum mean square error (MMSE), respectively. A low complexity semi-blind channel estimation [8] and a channel estimation employing reliable soft symbols [9] have been proposed. In [10], compressive sensing-based channel estimation and feedback overhead reduction technique is introduced. These approaches still use the same pilot duration for all users.

In this paper, we optimize the channel sensing duration for each user, extending [5] to downlink MU-MISO systems. Our main contributions are as follows: we propose a three-phase protocol, starting with (i) an initial beam sweeping, followed by (ii) an adaptive pilot duration per user, and finally (iii) data transmission. At each time slot in the second phase, we apply a new decision method that determines if a user should continue pilot transmission or move to the data transmission phase. The decision method is based on comparing the current effective rate with a predicted rate. In contrast to [5], the effective rate of each user is derived considering interference from other users, and the robust regularized zero-forcing (RRZF) [11] precoder and equal power allocation (EPA) are adopted to transmit pilot and data. Simulation results demonstrate that the proposed scheme has a higher sum rate compared to other schemes.

II. Downlink MU-MISO System Model in the Simultaneous Pilot and Data Transmission

We consider a downlink MU-MISO system where a single BS communicates with M users as shown in Fig. 1. Note that UE_m is the m-th user. We assume that the BS is equipped with a uniform linear array (ULA) of N_{T} antennas, and all users are equipped with a single antenna. There are feedback channels between each user and the BS. All channels are assumed to remain constant during a transmission frame of duration T_f. The narrow-band flat fading downlink channel $\mathbf{h}_m \in \mathbb{C}^{N_{\text{T}} \times 1}$ of the m-th user can be defined as [12]

$$\mathbf{h}_m = \sum_{l=1}^{L} \alpha_{m,l} \mathbf{a}_{\text{Tx}}(\theta_{m,l}), \tag{1}$$

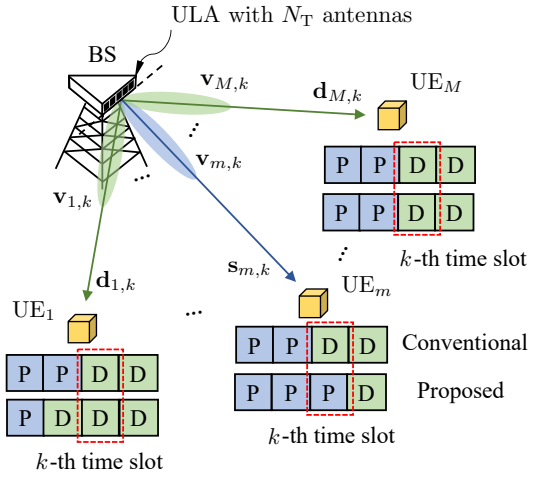

Fig. 1. An illustration of the comparison between the proposed scheme and conventional scheme in the mmWave MU-MISO downlink channel.

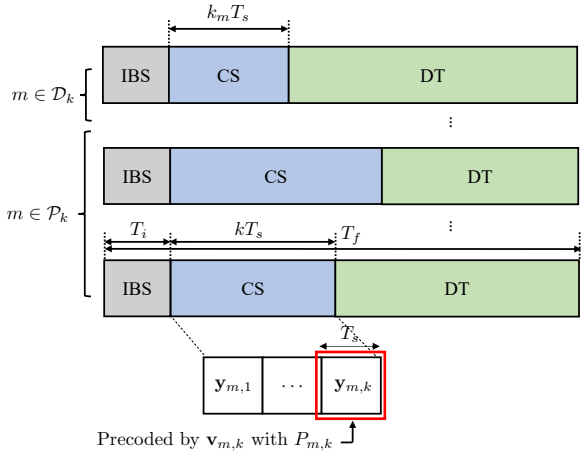

Fig. 2. Frame structure consisting of three phases [4] : initial beam sweeping (IBS), channel sensing (CS), data transmission (DT).

where $\alpha_{m,l}$ and $\theta_{m,l}$ are the complex channel gain and angle of departure (AoD) of the l-th path for the m-th user, respectively. For simplicity, the flat fading channel model is considered, however, the proposed scheme is applicable to the frequency selective channel model. The array vector $\mathbf{a}_{\mathrm{Tx}}(\theta_{m,l}) \in \mathbb{C}^{N_{\mathrm{T}}\times 1}$ is given by

$$\mathbf{a}_{\mathrm{Tx}}(\theta_{m,l}) = \left[1, e^{j\pi\cos\theta_{m,l}}, \ldots, e^{j\pi(N_{\mathrm{T}}-1)\cos\theta_{m,l}}\right]^{\mathrm{T}}. \quad (2)$$

As shown in Fig. 2, the frame duration T_f is divided into an initial beam sweeping (IBS) of duration T_i and an adaptive number of time slots with duration T_s containing Q sequential pilot transmission for channel sensing, while the remaining time is used for data transmission. For user m, the BS transmits pilots until time k_m which is determined by the proposed scheme as described in Sec. III-D, and the BS switches to data transmission (i.e., channel sensing duration is same as $k_m T_s$). Since the same Q pilot symbols are sent every time slot, channel sensing duration (time perspective) and channel estimation overhead (resource perspective) are linear. We consider the initial access where pilots are transmitted at the beginning of the frame [4]. After IBS, all users can belong to one of the two groups, which are pilot group $\mathcal{P}_k$ and data group $\mathcal{D}_k$: users that receive pilots from the BS at k-th time slot are in the pilot group $\mathcal{P}_k$, while users that receive the data from the BS are in the data group $\mathcal{D}_k$. In every time slot, users can be moved from $\mathcal{P}_k$ to $\mathcal{D}_k$, but not vice versa.

The received signal $\mathbf{y}_{m,k} \in \mathbb{C}^{Q\times 1}$ for user m during the k-th time slot is

$$\mathbf{y}_{m,k} = \begin{cases} \sqrt{P_{m,k}}\mathbf{h}_m^{\mathrm{H}}\mathbf{v}_{m,k}\mathbf{s}_{m,k} + \tilde{\mathbf{n}}_{m,k} & m \in \mathcal{P}_k, \\ \sqrt{P_{m,k}}\mathbf{h}_m^{\mathrm{H}}\mathbf{v}_{m,k}\mathbf{d}_{m,k} + \check{\mathbf{n}}_{m,k} & m \in \mathcal{D}_k, \end{cases} \quad (3)$$

where $P_{m,k}$ is the allocated power with $\sum_{m=1}^{M} P_{m,k} = P_{\mathrm{T}}$, the total transmit power at the BS; $\mathbf{v}_{m,k} \in \mathbb{C}^{N_{\mathrm{T}}\times 1}$ is the precoder (see Section III-C); $\mathbf{s}_{m,k} \in \mathbb{C}^{Q\times 1}$ ($\|\mathbf{s}_{m,k}\|^2 = Q$) is an orthogonal pilot sequence i.e., $\mathbf{s}_{m,k}^{\mathrm{H}}\mathbf{s}_{m',k} = 0$ for $m \neq m'$, $\mathbf{d}_{m,k} \in \mathbb{C}^{Q\times 1}$ ($\|\mathbf{d}_{m,k}\|^2 = Q$) is random data sequence. Finally, $\tilde{\mathbf{n}}_{m,k}$ and $\check{\mathbf{n}}_{m,k}$ denote noise and interference from other users $m' \in \mathcal{P}_k \cup \mathcal{D}_k \setminus \{m\}$. For any user $m \in \mathcal{P}_k$, we can find $y_{m,k} = \mathbf{s}_{m,k}^{\mathrm{H}}\mathbf{y}_{m,k}/\|\mathbf{s}_{m,k}\|^2$ leading to the following equation:

$$y_{m,k} = \sqrt{P_{m,k}}\mathbf{h}_m^{\mathrm{H}}\mathbf{v}_{m,k} + \tilde{n}_{m,k}, \quad m \in \mathcal{P}_k, \quad (4)$$

with $\tilde{n}_{m,k} \sim \mathcal{CN}(\mathbf{0}, \tilde{\sigma}_{m,k}^2)$, where $\tilde{\sigma}_{m,k}^2 = \sigma^2/Q + \sum_{m'\in\mathcal{D}_k} P_{m',k}\left|\mathbf{h}_m^{\mathrm{H}}\mathbf{v}_{m',k}\right|^2$.

III. Optimizing mmWave Channel Sensing Duration for Downlink MU-MISO System

At every time slot, the BS first determines the precoder and allocates the power to each user. Then, the BS computes the predicted rates for each user in the pilot group, and the predicted rates are compared with the current rates. If the predicted rate is lower than the current rate of a user, the user enters the data group and stops sending pilots.

A. Initial Beam Sweeping

In the initial beam sweeping phase, the BS sends out pilots consisting of Q consecutive symbols. In the course of the beam sweeping, each beamformer at the BS steers towards M_{T} equispaced directions within $[0, \pi]$. The beamformers $\bar{\mathbf{a}}_{\mathrm{Tx}}(\bar{\theta}, M_{\mathrm{T}}) \in \mathbb{C}^{M_{\mathrm{T}}\times 1}$ is given by [13]

$$\bar{\mathbf{a}}_{\mathrm{Tx}}(\bar{\theta}, M_{\mathrm{T}}) = \left[1, e^{j\pi\cos\bar{\theta}}, \ldots, e^{j\pi(M_{\mathrm{T}}-1)\cos\bar{\theta}}\right]^{\mathrm{T}}, \quad (5)$$

where $\bar{\theta}$ is a steering direction from the BS. Each user determines the beamformer maximizing the received power and feeds it back to the BS, which is used as initial precoder $\mathbf{v}_{m,1}$. Note that the BS uses M_{T} antennas which is smaller than N_{T} to reduce beam sweeping overhead (i.e., $M_{\mathrm{T}} \ll N_{\mathrm{T}}$).

B. Channel Sensing

At $(k-1)$-th time slot, a user $m \in \mathcal{P}_{k-1}$, uses its observations up to time $k-1$, $\mathbf{y}_{m,1:k-1} = [y_{m,1}, \ldots, y_{m,k-1}]^{\mathrm{T}}$, to provide a channel estimate

$$\hat{\mathbf{h}}_{m,k-1} = \arg\max_{\mathbf{h}_m} p(\mathbf{y}_{m,1:k-1}|\mathbf{h}_m), \quad m \in \mathcal{P}_{k-1}, \quad (6)$$

as well as a corresponding error covariance $\mathbf{C}_{m,k-1}$. Hence, after the $(k-1)$-th pilot transmission, the estimated channel $\hat{\mathbf{h}}_{m,k-1}$ of m-th user is distributed as $\hat{\mathbf{h}}_{m,k-1} \sim \mathcal{CN}(\mathbf{h}_m, \mathbf{C}_{m,k-1})$. This covariance information can be obtained from the Fisher information, as derived in Appendix A.

C. Robust Regularized Zero-forcing Precoding

Since the true channel is not given, the RRZF precoding is adopted to improve the performance of zero-forcing precoding. After the channel sensing at $(k-1)$-th time slot, the RRZF precoding is given by [11]:

$$\mathbf{V}_k = \hat{\mathbf{H}}_{k-1}\left(\hat{\mathbf{H}}_{k-1}^{\mathrm{H}}\hat{\mathbf{H}}_{k-1} + \sum_{m=1}^{M}\mathbf{C}_{m,k-1} + \frac{\sigma^2}{P_{\mathrm{T}}}\mathbf{I}\right)^{-1}, \quad (7)$$

where $\mathbf{V}_k = [\mathbf{v}_{1,k}, \cdots, \mathbf{v}_{M,k}] \in \mathbb{C}^{N_{\mathrm{T}}\times M}$ is precoding matrix, and $\hat{\mathbf{H}}_{k-1} = [\hat{\mathbf{h}}_{1,k-1}, \cdots, \hat{\mathbf{h}}_{M,k-1}] \in \mathbb{C}^{N_{\mathrm{T}}\times M}$ is estimated channel matrix.

D. Decision to Stop Pilot Transmissions

Before the pilot transmission, for users in $\mathcal{P}_{k-1}$, the BS determines whether to continue channel sensing or switches to data transmission by comparing the predicted rate $\hat{R}_{m,k}$ and the current rate $R_{m,k-1}$. The rate $R_{m,k-1}$ is the rate that is provided if the user switches to the set $\mathcal{D}_k$ and is given by [14]

$$R_{m,k-1} = \left(1 - \frac{T_i + (k-1)T_s}{T_f}\right)\log_2\left(1+\gamma_{m,k-1}\right), \quad m \in \mathcal{P}_{k-1}, \quad (8)$$

where

$$\gamma_{m,k-1} = \frac{P_{m,k}|\hat{\mathbf{h}}_{m,k-1}^{\mathrm{H}}\mathbf{v}_{m,k}|^2}{\sigma^2 + \sum_{m'\in\mathcal{D}_{k-1}} P_{m',k}|\hat{\mathbf{h}}_{m,k-1}^{\mathrm{H}}\mathbf{v}_{m',k}|^2 + \sigma^2_{\mathrm{e},m,k-1}(\mathbf{V}_k,\mathbf{p}_k)}, \quad (9)$$

in which $\mathbf{p}_k = [P_{1,k},\ldots,P_{M,k}]^{\mathrm{T}}$ is the power allocation at k-th time slot, while the channel estimation error can be described as

$$\sigma^2_{\mathrm{e},m,k-1}(\mathbf{V}_k,\mathbf{p}_k) = \sum_{i\in\{m\}\cup\mathcal{D}_{k-1}} P_{i,k}\mathbf{v}_{i,k}^{\mathrm{H}}\mathbf{C}_{m,k-1}\mathbf{v}_{i,k}. \quad (10)$$

where is a function of the channel error covariance $\mathbf{C}_{m,k-1}$. Computation of the channel error covariance $\mathbf{C}_{m,k-1}$ is described in Appendix A. Note that the channel estimation error $\sigma^2_{\mathrm{e},m,k-1}(\mathbf{V}_k,\mathbf{p}_k)$ decreases with the time slot index k as the FIM relies on a greater number of pilot transmissions as shown in Appendix A.

The rate $\hat{R}_{m,k}$ is the predicted rate if the m-th user defers switching to the set $\mathcal{D}_k$ and continues with one more pilot transmission. It is given by

$$\hat{R}_{m,k} = \left(1 - \frac{T_i + kT_s}{T_f}\right)\log_2(1+\hat{\gamma}_{m,k}), \quad m \in \mathcal{P}_{k-1}, \quad (11)$$

where we note the reduction in the pre-log factor and define

$$\hat{\gamma}_{m,k} = \frac{P_{m,k}|\hat{\mathbf{h}}_{m,k-1}^{\mathrm{H}}\mathbf{v}_{m,k}|^2}{\sigma^2 + \sum_{m'\in\mathcal{D}_{k-1}} P_{m',k}|\hat{\mathbf{h}}_{m,k-1}^{\mathrm{H}}\mathbf{v}_{m',k}|^2 + \hat{\sigma}^2_{\mathrm{e},m,k}(\mathbf{V}_k,\mathbf{p}_k)}, \quad (12)$$

in which the predicted channel estimation error

$$\hat{\sigma}^2_{\mathrm{e},m,k}(\mathbf{V}_k,\mathbf{p}_k) = \sum_{i\in\{m\}\cup\mathcal{D}_{k-1}} P_{i,k}\mathbf{v}_{i,k}^{\mathrm{H}}\hat{\mathbf{C}}_{m,k}\mathbf{v}_{i,k}, \quad (13)$$

is a function of the predicted channel error covariance $\hat{\mathbf{C}}_{m,k}$, whose computation is described in Appendix B.

Algorithm 1 Optimizing channel sensing duration scheme in downlink MU-MISO systems

Initialization:
$\mathbf{v}_{m,1} = \bar{\mathbf{a}}_{\mathrm{Tx}}(\bar{\theta}_m, M_{\mathrm{T}})$, $P_{m,1} = P_{\mathrm{T}}/M$, $\forall m$
$\mathcal{P}_1 = \{1,\ldots,M\}$, $\mathcal{D}_1 = \emptyset$
Downlink transmission with observation $\mathbf{y}_{m,1}$ from (3)
for $k = 2, 3, \ldots$ **do**
  Estimate the channel using (6) for users $m \in \mathcal{P}_{k-1}$
  Compute the RRZF precoder $\mathbf{V}_k$ from (7)
  for $m \in \mathcal{P}_{k-1}$ **do**
    Compute the current rate $R_{m,k-1}$ from (8)
    Compute the predicted rate $\hat{R}_{m,k}$ from (11)
    if $\hat{R}_{m,k} > R_{m,k-1}$ **then**
      place user m in $\mathcal{P}_k$
    else
      place user m in $\mathcal{D}_k$
    end if
  end for
  Downlink transmission with observation $\mathbf{y}_{m,k}$ from (3)
end for

Finally, the decision rule is as follows:

- If $\hat{R}_{m,k} \geq R_{m,k-1}$, user m stays in the pilot set ($m \in \mathcal{P}_k$) and the BS transmits pilot with $\mathbf{v}_{m,k}$ and $P_{m,k}$, estimates the channels by calculating the $\mathbf{C}_{m,k}$ with consecutive observations $\mathbf{y}_{m,1:k}$ and then updates $\mathbf{v}_{m,k+1}$ and $P_{m,k+1}$.
- If $\hat{R}_{m,k} < R_{m,k-1}$, the BS keeps $\mathbf{v}_{m,k}$ and $P_{m,k}$ and switches to data transmission with rate $R_{m,k-1}$ ($m \in \mathcal{D}_k$).

Then the decision process is repeated at $(k+1)$-th time slot. A summary of the proposed scheme is presented in Algorithm 1.

In relation to the complexity of the proposed scheme, most procedures of the proposed scheme are generally performed in a base station where computational complexity is not a problem. In addition, the proposed scheme includes operations commonly considered in a wide range of communication algorithms such as beamformer design and CRB calculation. Therefore, the proposed scheme is considered to be practical.

E. Power Allocation

Determining an optimal power allocation is complicated since the number of data transmitting users is continually

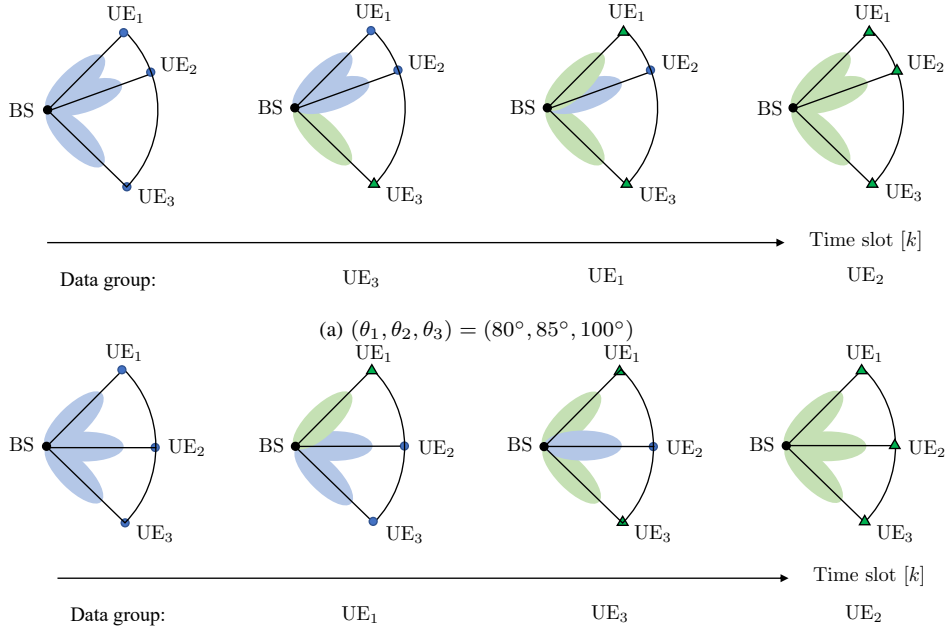

(a) $(\theta_1, \theta_2, \theta_3) = (80°, 85°, 100°)$

(b) $(\theta_1, \theta_2, \theta_3) = (80°, 90°, 100°)$

Fig. 3. Two representative examples of three users in the downlink MU-MISO systems (blue: pilot group, green: data group). In the figure on the left, user 3 first joins $\mathcal{D}_k$ at $k = 7$, followed by user 1 at $k = 10$ and finally user 2 at $k = 16$.

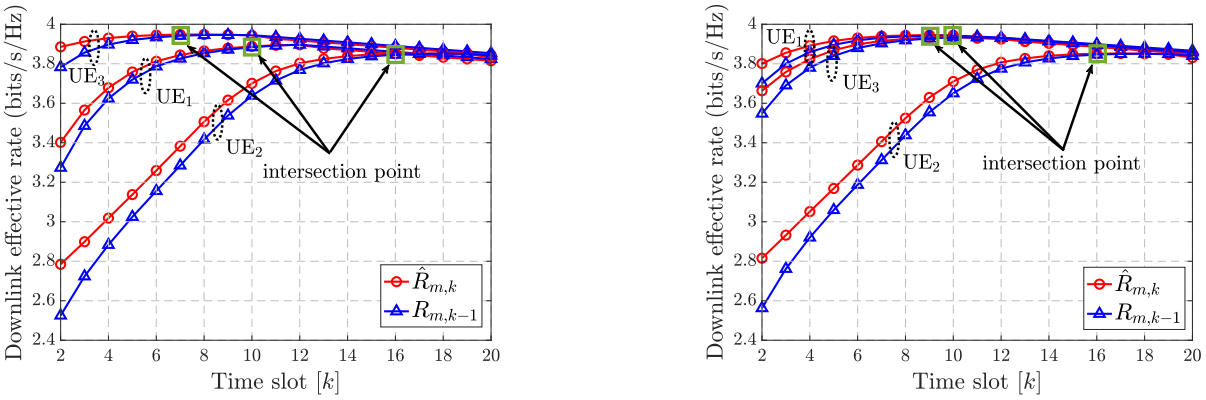

(a) $(\theta_1, \theta_2, \theta_3) = (80°, 85°, 100°)$

(b) $(\theta_1, \theta_2, \theta_3) = (80°, 90°, 100°)$

Fig. 4. The comparison between the predicted rate $\hat{R}_{m,k}$ and the current rate $R_{m,k-1}$ with the time slot in the representative examples.

changing. Upon completion of Algorithm 1 (i.e., at the first time k' for which $\mathcal{P}_{k'} = \emptyset$), the power allocation that maximizes the signal to interference plus noise ratio (SINR) can be used [15]. It is the solution of the following problem:

$$\max_{\mathbf{p}_{k'}} \quad \sum_{m=1}^{M} \log_2 (1 + \gamma_{m,k'}) \tag{14}$$

$$\text{s.t.} \quad \mathbf{p}_{k'} \geq 0, \mathbf{1}^{\mathrm{T}} \mathbf{p}_{k'} \geq P_{\mathrm{T}} \tag{15}$$

$$\gamma_{m,k'} = \frac{P_{m,k'} |\hat{\mathbf{h}}_{m,k'}^{\mathrm{H}} \mathbf{v}_{m,k'}|^2}{\sigma^2 + \sum_{m' \neq m} P_{m',k} |\hat{\mathbf{h}}_{m,k'}^{\mathrm{H}} \mathbf{v}_{m',k'}|^2}, \tag{16}$$

which can be obtained iteratively, starting from a uniform allocation [15]. Hence, since the above optimization is only applicable after the completion of the proposed scheme, we proposed to use equal power allocation at the BS, $P_{m,k} = P_{\mathrm{T}}/M$ for $k < k'$.

IV. Simulation Results and Discussions

In this section, the performance of the proposed scheme is evaluated for different parameters are presented.

A. Simulation Settings

We consider MU-MISO system consisting of a BS with $N_{\mathrm{T}} = 60$ and M single-antenna users. We set the transmitted signal-to-noise-ratio (SNR) $P_{\mathrm{T}}/\sigma^2 = 5$ dB and $L = 2$ where one dominant path and one secondary path exist, and the power of the secondary path is 10 dB lower than the power of the dominant path [16]. Note that the dominant path is line-of-sight (LoS) between BS and user, and the secondary path is

uniformly distributed within $[0°, 180°]$. In Fig. 2, the frame structure is comprised of 500 time slots i.e., $T_f = 500T_s$ and each time slot consists of $Q = 139$ symbols. For the initial beam sweeping, we set $M_{\mathrm{T}} = 8$, so the time period of beam sweeping is $T_i = 8T_s$.

B. Two Representative Examples of Three Users Case

Fig. 3 shows two representative examples when a BS communicates with $M = 3$ users. In Fig. 3, the BS transmits the pilots to blue users which are in the pilot group and data to green users which are in the data group, respectively. Fig. 4 shows the comparison between the predicted rate $\hat{R}_{m,k}$ and the current rate $R_{m,k-1}$ with the time slot for representative examples: $\hat{R}_{m,k}$ and $R_{m,k-1}$ are concave because the channel sensing duration is optimized at the maximum point of the effective rate and then the effective rate decreases due to excessive pilot transmission. As expected, conversion to data group is performed in the order of UE_3, UE_1, and UE_2 in Fig. 4 (a), and in order of UE_1, UE_3, and UE_2 in Fig. 4 (b), respectively. In Fig. 4 (a), UE_3 is mostly separated from other users, resulting in the least impact of interference, and achieves the highest effective rate. As the interference is decreased, higher initial rates can be achieved with a relatively small number of pilot transmissions, which leads to an early end of pilot transmissions (see the intersection points). Conversely, UE_2 is most affected by interference, achieving a lower effective rate and requires more pilot transmissions. In Fig. 4 (b), UE_2, which is most affected by interference, achieves the lowest effective rate and switches to data transmission lastly. Note that although UE_1 and UE_3 are affected by the same interference, an initial effective rate difference occurs due to a difference in initial channel sensing accuracy. As shown in Fig. 4 (a) and Fig. 4 (b), as the channel sensing duration becomes longer, the interference term becomes small, because the channel sensing is more accurate and the precoder is well designed accordingly.

C. Downlink Sum Rate with Different Numbers of UEs

In Fig. 5, we compare the proposed scheme to the $R_{k=10}$ (i.e., using a fixed number of 10 pilot slots), $R_{k=20}$, $R_{k=40}$, and $R_{k=60}$ with different number of users M. The downlink sum rate R_k can be defined as [14]

$$R_k = \sum_{m=1}^{M} R_{m,k}. \tag{17}$$

As the number of users increases, the downlink sum rate increases. As expected, the proposed scheme is always higher than the $R_{k=10}$, $R_{k=20}$, $R_{k=40}$, and $R_{k=60}$, as shown in Fig. 5. As the number of users increases, the optimal channel sensing duration increases, so it can be seen that $R_{k=60}$ is the largest one for the high M regime. Conversely, as the number of users decreases, the optimal channel sensing duration decreases, so $R_{k=10}$ is the largest one for the low M regime. For the high M regime, the difference in the optimal channel sensing duration between users becomes larger, so the performance due to the proposed algorithm is further improved compared to $R_{k=10}$, $R_{k=20}$, $R_{k=40}$, and $R_{k=60}$.

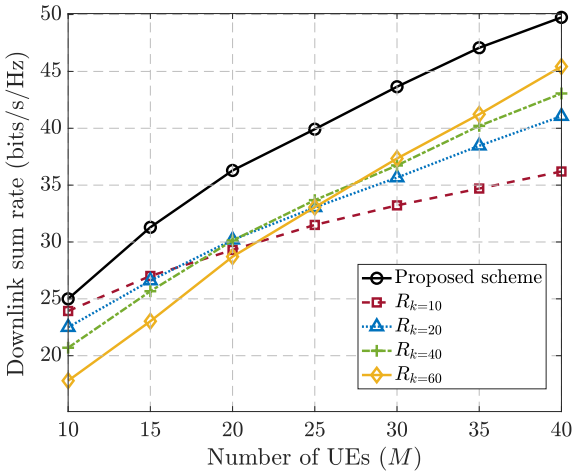

Fig. 5. Downlink sum rate achieved by the proposed scheme vs. a fixed number of pilot slots (10 for $R_{k=10}$, 20 for $R_{k=20}$, 40 for $R_{k=40}$, and 60 for $R_{k=60}$) with different number of users M.

V. Conclusions

For MU-MISO systems, we have proposed an adaptive scheme that optimizes the channel sensing duration of each user to reduce the channel estimation overhead. Before the pilot transmission, the BS predicts the effective rate with pre-defined precoder and allocated power and decide which user stops pilot transmission and switch to data transmission. Numerical experiments have shown that the proposed scheme has a higher sum rate compared to the other scheme, which estimates the channel in the same duration for all users. In the future, joint user selection, precoding, and power allocation optimization, which maximizes the sum rate, will be investigated.

VI. Acknowledgements

This work was supported by Institute of Information & communications Technology Planning & Evaluation (IITP) grant funded by the Korea government (NFA) (No.2019-0-01325, Developed of wireless communication tracking based location information system in disaster scene for fire-fighters and person who requested rescue), Spanish Research Agency grant PID2020-118984GB-I00, and by the Swedish Research Council, under grant 2018-03701.

Appendix A
Computation of the Channel Error Covariance

We introduce the noise-free observation

$$\mu_{m,k} = \sqrt{P_{m,k}} \sum_{l=1}^{L} \alpha_{m,l} \mathbf{a}_{\mathrm{Tx}}^{\mathrm{H}}(\theta_{m,l}) \mathbf{v}_{m,k}, \tag{18}$$

and the unknown channel parameter vector $\boldsymbol{\eta}_m \in \mathbb{R}^{3L\times 1}$ of m-th user can be defined as

$$\boldsymbol{\eta}_m = \left[\boldsymbol{\eta}_{m,1}^{\mathrm{T}}, \cdots, \boldsymbol{\eta}_{m,L}^{\mathrm{T}}\right]^{\mathrm{T}}, \tag{19}$$

in which $\boldsymbol{\eta}_{m,l} \in \mathbb{R}^{3\times 1}$ consists of the channel parameters (channel gain and AoD) for the l-th path

$$\boldsymbol{\eta}_{m,l} = \left[\theta_{m,l}, \Re\alpha_{m,l}, \Im\alpha_{m,l}\right]^{\mathrm{T}}, \tag{20}$$

where $\Re\alpha_{m,l}$ is real part and $\Im\alpha_{m,l}$ is imaginary part of the channel gain $\alpha_{m,l}$.

A. Error covariance of $\boldsymbol{\eta}_m$

Let $\hat{\boldsymbol{\eta}}_{m,k-1}$ be the estimate of $\boldsymbol{\eta}_m$ at $(k-1)$-th time slot (e.g., obtained by the maximum likelihood (ML) estimator), then the error covariance is bounded as

$$\mathbb{E}_{\boldsymbol{\eta}_m}\left[\left(\hat{\boldsymbol{\eta}}_{m,k-1} - \boldsymbol{\eta}_m\right)\left(\hat{\boldsymbol{\eta}}_{m,k-1} - \boldsymbol{\eta}_m\right)^{\mathrm{T}}\right] \succeq \mathbf{J}_{\boldsymbol{\eta}_m}^{-1}, \tag{21}$$

in which $\mathbf{J}_{\boldsymbol{\eta}_m} \in \mathbb{R}^{3L\times 3L}$ is the Fisher information matrix (FIM). The FIM $\mathbf{J}_{\boldsymbol{\eta}_m}$ is defined as

$$\mathbf{J}_{\boldsymbol{\eta}_m} \triangleq -\mathbb{E}\left[\frac{\partial^2 \ln f\left(\mathbf{y}_{m,1:k-1}|\boldsymbol{\eta}_m\right)}{\partial\boldsymbol{\eta}_m \partial\boldsymbol{\eta}_m^{\mathrm{T}}}\right], \tag{22}$$

where $\ln f\left(y_{m,1:k-1}|\boldsymbol{\eta}_m\right)$ is log-likelihood function of the consecutive observations up to $(k-1)$-th time slot conditioned on $\boldsymbol{\eta}_m$. Since these observations are conditionally independent, $\ln f\left(\mathbf{y}_{m,1:k-1}|\boldsymbol{\eta}_m\right) = \sum_{k'=1}^{k-1} \ln f\left(y_{m,k'}|\boldsymbol{\eta}_m\right)$ in which

$$\ln f\left(y_{m,k'}|\boldsymbol{\eta}_m\right) \propto -\frac{1}{\tilde{\sigma}_{m,k}^2}\left|y_{m,k'} - \mu_{m,k'}\right|^2, \tag{23}$$

where $\mu_{m,k'} = \sqrt{P_{m,k'}}\mathbf{h}_m^{\mathrm{H}}\mathbf{v}_{m,k'}$ and $\mathbf{J}_{\boldsymbol{\eta}_m}$ can be easily computed, following the approach in [17]. Since the FIM depends on the true channel parameters $\boldsymbol{\eta}_m$, which are not known, $\hat{\boldsymbol{\eta}}_{m,k-1}$ is used to evaluate the FIM, denoted as $\mathbf{J}_{\boldsymbol{\eta}_m=\hat{\boldsymbol{\eta}}_{m,k-1}}(\mathbf{V}_{1:k-1}, \mathbf{p}_{1:k-1})$, accumulated from $y_{m,1}$ (transmitted by $\mathbf{V}_1$, $\mathbf{p}_1$) to $y_{m,k-1}$ (transmitted by $\mathbf{V}_{k-1}$, $\mathbf{p}_{k-1}$). The corresponding error covariance is then $\mathbf{J}^{-1}_{\boldsymbol{\eta}_m=\hat{\boldsymbol{\eta}}_{m,k-1}}(\mathbf{V}_{1:k-1}, \mathbf{p}_{1:k-1})$.

B. Error covariance of $\mathbf{C}_{m,k-1}$

The error covariance matrix $\mathbf{C}_{m,k-1}$ of $\mathbf{h}_m \in \mathbb{C}^{N_{\mathrm{T}}\times 1}$ can be calculated by a Jacobian transformation matrix $\mathbf{T}_m \in \mathbb{C}^{N_{\mathrm{T}}\times 3L}$:

$$\mathbf{C}_{m,k-1} = \mathbf{T}_m \mathbf{J}^{-1}_{\boldsymbol{\eta}_m=\hat{\boldsymbol{\eta}}_{m,k-1}}(\mathbf{V}_{1:k-1}, \mathbf{p}_{1:k-1})\mathbf{T}_m^{\mathrm{H}}, \tag{24}$$

where the transformation matrix $\mathbf{T}_m$ is

$$\mathbf{T}_m = \left.\frac{\partial \mathbf{h}_m}{\partial \boldsymbol{\eta}_m}\right|_{\boldsymbol{\eta}_m=\hat{\boldsymbol{\eta}}_{m,k-1}} \in \mathbb{C}^{N_{\mathrm{T}}\times 3L}. \tag{25}$$

The entries in $\mathbf{T}_m$ can be computed from the relations

$$\frac{\partial \mathbf{h}_m}{\partial \theta_{m,l}} = \alpha_{m,l}\dot{\mathbf{a}}_{\mathrm{Tx}}\left(\theta_{m,l}\right), \tag{26}$$

$$\frac{\partial \mathbf{h}_m}{\partial \Re\alpha_{m,l}} = \mathbf{a}_{\mathrm{Tx}}(\theta_{m,l}), \tag{27}$$

$$\frac{\partial \mathbf{h}_m}{\partial \Im\alpha_{m,l}} = j\mathbf{a}_{\mathrm{Tx}}(\theta_{m,l}). \tag{28}$$

APPENDIX B
COMPUTATION OF THE PREDICTED CHANNEL ERROR COVARIANCE

The prediction of the channel error covariance that would result after the transmission of pilots in the k-th time slot can be found as

$$\hat{\mathbf{C}}_{m,k} = \mathbf{T}_m \mathbf{J}^{-1}_{\boldsymbol{\eta}_m=\hat{\boldsymbol{\eta}}_{m,k-1}}(\mathbf{V}_{1:k}, \mathbf{p}_{1:k})\mathbf{T}_m^{\mathrm{H}}, \tag{29}$$

where the only difference with respect to (24) is that we account for the FIM from one additional pilot transmission.

REFERENCES

[1] F. Liu, Y. Cui, C. Masouros, J. Xu, T. X. Han, Y. C. Eldar, and S. Buzzi, "Integrated sensing and communications: Towards dual-functional wireless networks for 6G and beyond," *arXiv preprint arXiv:2108.07165*, 2021.

[2] Z. Wan, Z. Gao, C. Masouros, D. W. K. Ng, and S. Chen, "Integrated sensing and communication with mmWave massive MIMO: A compressed sampling perspective," *arXiv preprint arXiv:2201.05766*, 2022.

[3] G. Wunder, S. Stefanatos, A. Flinth, I. Roth, and G. Caire, "Low-overhead hierarchically-sparse channel estimation for multiuser wideband massive MIMO," *IEEE Trans. Wireless Commun.*, vol. 18, no. 4, pp. 2186–2199, Apr. 2019.

[4] H. Shokri-Ghadikolaei, L. Gkatzikis, and C. Fischione, "Beam-searching and transmission scheduling in millimeter wave communications," in *Proc. IEEE Int. Conf. Commun. (ICC)*, Jun. 2015, pp. 1292–1297.

[5] J. Kang, N. Garcia, H. Wymeersch, C. Fischione, G. Seco-Granados, and S. Kim, "Optimizing the mmwave channel estimation duration by rate prediction," *IEEE Commun. Lett.*, vol. 25, no. 2, pp. 555–559, 2021.

[6] A. Adhikary, J. Nam, J. Ahn, and G. Caire, "Joint spatial division and multiplexingthe large-scale array regime," *IEEE Trans. Inf. Theory*, vol. 59, no. 10, pp. 6441–6463, 2013.

[7] X. Rao and V. K. N. Lau, "Distributed compressive CSIT estimation and feedback for FDD multi-user massive MIMO systems," *IEEE Trans. Signal Process.*, vol. 62, no. 12, pp. 3261–3271, 2014.

[8] D. De Donno, J. Palacios, and J. Widmer, "Millimeter-wave beam training acceleration through low-complexity hybrid transceivers," *IEEE Trans. Wireless Commun.*, vol. 16, no. 6, pp. 3646–3660, 2017.

[9] S. Park, J. W. Choi, J. Seol, and B. Shim, "Expectation-maximization-based channel estimation for multiuser MIMO systems," *IEEE Trans. Commun.*, vol. 65, no. 6, pp. 2397–2410, 2017.

[10] A. Mayouche, A. Metref, and J. Choi, "Downlink training overhead reduction technique for FDD massive MIMO systems," *IEEE Signal Process. Lett.*, vol. 25, no. 8, pp. 1201–1205, 2018.

[11] Z. Wang and W. Chen, "Regularized zero-forcing for multiantenna broadcast channels with user selection," *IEEE Wireless Commun. Lett.*, vol. 1, no. 2, pp. 129–132, 2012.

[12] R. W. Heath, N. Gonzlez-Prelcic, S. Rangan, W. Roh, and A. M. Sayeed, "An overview of signal processing techniques for millimeter wave MIMO systems," *IEEE J. Sel. Topics Signal Process.*, vol. 10, no. 3, pp. 436–453, Feb. 2016.

[13] V. Desai, L. Krzymien, P. Sartori, W. Xiao, A. Soong, and A. Alkhateeb, "Initial beamforming for mmWave communications," in *Proc. IEEE Asilomar Conf. Signal Syst. Comput.*, 2014, pp. 1926–1930.

[14] S. Vishwanath, N. Jindal, and A. Goldsmith, "Duality, achievable rates, and sum-rate capacity of Gaussian MIMO broadcast channels," *IEEE Trans. Inf. Theory*, vol. 49, no. 10, pp. 2658–2668, 2003.

[15] M. Lee and S. K. Oh, "A simplified iterative water-filling algorithm for per-user power allocation in multiuser MMSE-precoded MIMO systems," in *Proc. IEEE Veh. Tech. Conf. (VTC)*, 2008, pp. 744–748.

[16] M. K. Samimi and T. S. Rappaport, "3-D millimeter-wave statistical channel model for 5G wireless system design," *IEEE Trans. Microw. Theory Techn.*, vol. 64, no. 7, pp. 2207–2225, Jul. 2016.

[17] N. Garcia, H. Wymeersch, and D. T. M. Slock, "Optimal precoders for tracking the AoD and AoA of a mmWave path," *IEEE Trans. Signal Process.*, vol. 66, no. 21, pp. 5718–5729, Nov. 2018.